Introduction

Quentin Bone and Linda Maddock

Marine Biological Association, The Laboratory, Citadel Hill,
Plymouth, PL1 2PB

Aquatic organisms swim in a variety of ways, from jet propulsion to ciliary action; they swim at a wide range of speeds and span a vast size range, from bacteria and protists, to the largest whales. In consequence of the enormous size and speed range of swimming organisms, they operate under notably different Reynolds number regimes. This has led to very different selection pressures in different forms, and one of the fascinating aspects of aquatic locomotion is the remarkable sets of adaptations that have been evolved for different purposes. These are seen not only in external form, as in the body shapes of fish, penguins, and fossil marine reptiles, but also in the way the locomotor muscles are designed and controlled, and in the structure of the skeleton.

The different chapters consider some of the problems faced by swimmers from several points in the vast array of aquatic organisms, from the biological and physical effects determining the patterns of bacterial populations, to the remarkable special adaptations of penguins for underwater 'flight'. All organisms are constructed from materials that are denser than the water in which they swim. To avoid sinking either they must use buoyancy strategies, such as changing in shape, as do some marine protists, or storing light materials (like fat or gas) to provide static lift, or they must generate dynamic lift, as ichthyosaurs apparently did. Most fishes and all aquatic tetrapods have gas-filled swim bladders or lungs and hence are close to neutral buoyancy (at least at a particular depth). Some tetrapods, however, like penguins and plesiosaurs, can apparently achieve neutral buoyancy only by swallowing stones as ballast.

Although much can be inferred about the modes of life of fossil aquatic reptiles by consideration of living aquatic tetrapods, they are regrettably unavailable for observation and experiment, and it is with fishes (and their competitors, the squids) that most is known of the operation and control of the locomotor systems.

Squid are renowned for their jet propulsion, but their fins play an important and much less well known role in swimming. Like terrestrial animals, fish can move at different

2   Q. Bone and L. Maddock

speeds, and the introduction of the concept of gaits to fish swimming (from terrestrial animal locomotion studies), provides a new approach to fish swimming. The great majority of fish swim by oscillating the body with the myotomal muscles, and there has been considerable interest recently in the way that the control and timing of contraction of these segmental muscles is brought about. This has been examined in detail theoretically and experimentally, as have the concomitant physiological adaptations of the circulatory and respiratory systems in fast-swimming fish. Earlier experimental work on the physiology of swimming in fish involved small fish in relatively small flumes or tunnel respirometers. The development of a large portable high-speed water tunnel respirometer has enabled this approach to be extended to the most active fish, such as tunas and sharks.

Not all aspects of the biology of aquatic animal locomotion are considered in this book. The chapters range from bacteria and protist swimming and buoyancy, to underwater 'flight' by penguins, and formation swimming on the surface by ducklings, via squid, fish and fossil reptiles, and the reader will find a wide variety of approaches to the problems, common to all aquatic organisms, of moving through water and avoiding sinking.

This volume has chapters from many of the contributors to a symposium meeting with the same title, held at Plymouth in 1991, under the joint auspices of the Marine Biological Association of the United Kingdom, and the Society for Experimental Biology. Quentin Bone is grateful to the Leverhulme Trust for the award of an Emeritus Fellowship, during the tenure of which he edited this book. We thank all those who contributed to the success of the original meeting, and to the production of this volume. Tracie Endicott and Adrian Bonsey provided invaluable assistance with the editing and preparation of the camera-ready copy.

Chapter 1

Functional patterns of swimming bacteria

J.O. KESSLER*[†], M.A. HOELZER[‡], T.J. PEDLEY* AND N.A. HILL*

*Department of Applied Mathematical Studies, The University, Leeds, LS2 9JT, UK
[†]Department of Physics, University of Arizona, Tucson, AZ 85721, USA
[‡]Department of Biology, The University of Alaska, Anchorage, AK 99508, USA

Concentrated populations of the aerobic swimming bacteria *Bacillus subtilis* rapidly use up the oxygen dissolved in their culture medium. As a result, oxygen diffuses in from the air interface, creating an upward concentration gradient. The organisms then swim towards the surface where they accumulate. Because this arrangement of mass density is unstable, the entire fluid culture convects. Biological and physical factors thus jointly serve to organize the population, yielding dynamics which greatly improve the transport and mixing of oxygen and the viability of the cells.

INTRODUCTION

Concentrated fluid cultures of swimming bacterial cells, such as motile strains of *Bacillus subtilis*, often form patterns (Kessler, 1989; Pfennig, 1962). They are easy to see when the fluid layer is shallow, and when the illumination provides adequate contrast. These patterns are fairly regular arrays of dots or stripes whose overall diameters and spacings are usually of order millimetres (Figure 1), i.e. much greater than the size of individual cells, typically micrometres. The pattern dimensions are also much greater than the average spacing between cells ($\sim 10^{-3}$ cm). What is seen are marked fluctuations in concentration $n(\mathbf{r},t)$ of bacterial cells, as discussed in Appendix 1. Generally, high cell concentrations are associated with, and cause, downward motion of the suspending fluid. However, the velocity of the fluid, $\mathbf{u}(\mathbf{r},t)$, is correlated with both local and remote values of $n(\mathbf{r},t)$. The relations between cell concentration, mean density of the fluid and convection are also discussed in Appendix 1.

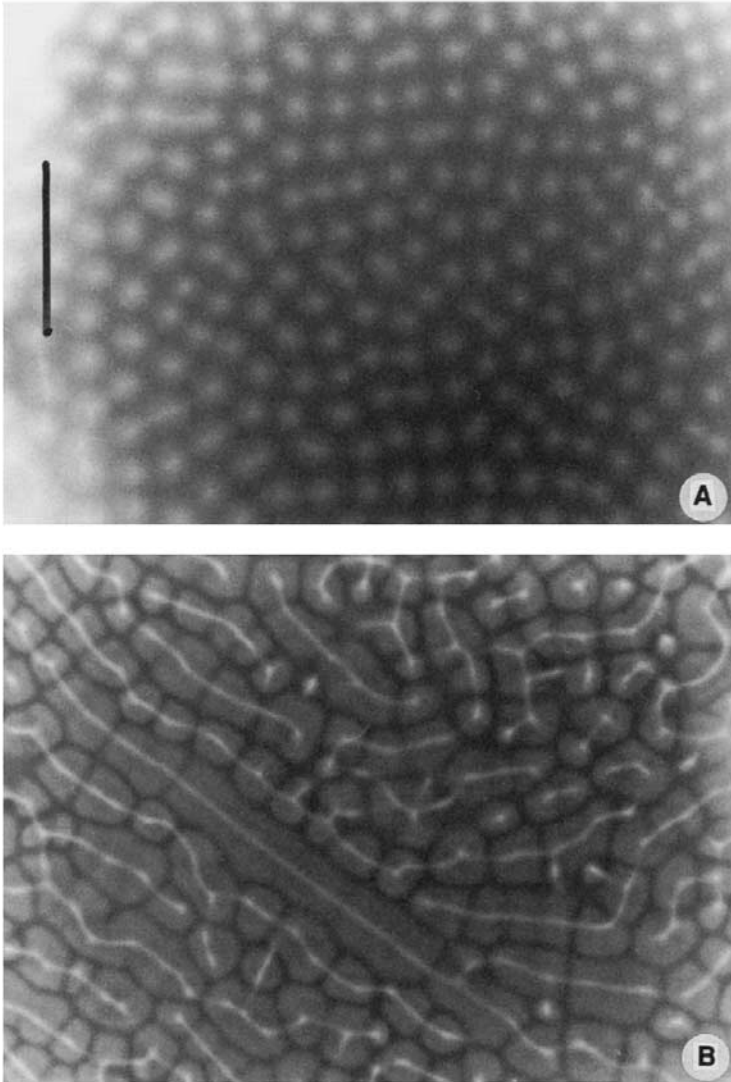4   J.O. Kessler, M.A. Hoelzer, T.J. Pedley and N.A. Hill

Figure 1. Bacterial concentration convection patterns seen in plan view. Dark-field illumination causes regions which contain many cells to appear white; there are fewer cells in the dark regions. (A) The fluid depth is approximately 2 mm. Scale bar: 1 cm. (B) Fluid depth 3 mm. The pattern geometry markedly depends on depth.

   Physical and biological factors combine to convert an originally static microbial habitat, e.g. a quiescent fluid bacterial culture in a petri dish, into a functional dynamic system. The sequence of events leading to pattern formation is ordered, first static and then dynamic. Eventually all the ingredient phenomena occur simultaneously. Oxygen is consumed by the bacteria and supplied from the air at the surface of the culture. Thus the oxygen concentration decreases downwards from the surface. As consumption

progresses the oxygen gradient steepens. The bacterial cells located within this gradient swim upwards, towards the air. Oxygen diffusion is usually too slow to reach the lower regions of the fluid. As the cells near the bottom deplete the supply, they stop swimming. The physiological components of pattern generation are respiration and oxygentaxis. Physical factors are the location of the surface, due to gravity, and the diffusion rate of oxygen.

Initially there is no general motion of the fluid, except for the slight local fluctuations that accompany the passage of a swimming organism. As the upward swimming of the bacteria towards the air progresses, the mean density of the increasingly cell-laden fluid strata next to the surface surpasses a stability threshold. The dense fluid layer then coalesces into descending plumes. The downward motion of dense fluid is necessarily coupled with the ascent of an exactly equal volume of fluid from below. This convective motion of the fluid and its occupants, driven by them, continues for hours or days, until the culture as a whole becomes senescent.
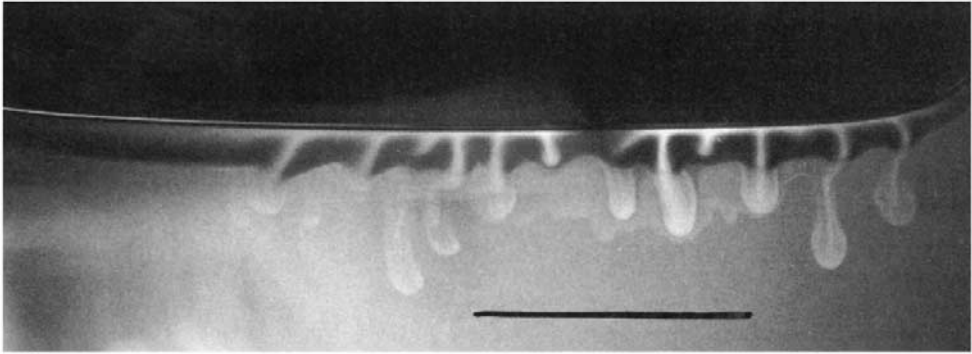

Figure 2. Concentration-convection pattern seen from the side. Air over the fluid interface. New plumes are starting while previous plumes penetrate the fluid below. The dark region between the interface and the main body of fluid is depleted of the cells which have swum to the surface. Dark-field. Scale bar: 1 cm.

Consumption and upward swimming have been recognized as 'biological'. The rest of the complex dynamics just described, the convection of fluid and the associated transport mechanisms, are entirely 'physical'. Nevertheless, there are remarkable biological consequences. There are direct benefits to the cell population in the form of an increased viability of an 'average cell'. Without convective mixing and transport, the large fraction of the cell population that is well below the surface becomes non-motile due to lack of oxygen. In contrast, in the early stages of the convection pattern, the stream carries downwards a high concentration of well-aerated bacteria, together with dissolved oxygen. This bacteria- and oxygen-transporting stream is to be seen in Figure 2 as a set of descending plumes. The displaced fluid that moves upwards is oxygen depleted and carries along some of the anoxic cells from below. Eventually, when convection is in full swing, most of the cells are again fully motile, except in the lowest strata where there is almost no movement.

6   J.O. Kessler, M.A. Hoelzer, T.J. Pedley and N.A. Hill

EXPERIMENTAL

Two strains of motile wild-type *Bacillus subtilis* were grown in enriched minimal medium, at 37° C, in glass flasks mounted on a shaker. When the cell concentration n was sufficient, usually $n \geq 5 \times 10^8$ cells cm^{-3}, patterns formed spontaneously a few minutes after shaking ceased. Generally, patterns were observed by dark-field illumination at room temperature, in a shallow layer of fluid culture. The pattern geometry was rather depth-dependent. No patterns occurred for fluid layers shallower than ~1 mm. In thick layers the patterns could not be seen in plan view, due to excessive light scatter by the bacterial population. The time lag between first pouring the fluid culture into a diagonally illuminated petri dish and the initial observation of patterns ranged from 30 s to 5 min, apparently depending mainly on the cell concentration and the aeration of the fluid.

To understand better the relationship between upward swimming and the patterns, another geometry was employed. Normally a bacterial culture a few millimetres deep is placed in a flat-bottomed petri dish, permitting the observation of the patterns which arise in shallow fluid layers. The new geometry consisted of a cuvette constructed of two microscope slides set on edge, separated by a 1-mm thick spacer at the bottom and side edges, then sealed with silicone grease. The bacterial culture, approximately 1 cm deep, could now be observed from the side (Figure 2). It was found that, soon after the cuvette was filled, a region about 1 mm below the air/fluid interface became depleted of bacteria because they swam towards the interface. This cell accumulation at the meniscus then became gravitationally unstable. Plumes of fluid that contained many more than the overall volume-averaged number of cells then slowly began to descend downwards from the interface.

These horizontally observed cell-concentration-driven convection plumes (Figure 2) do not correspond exactly to a side view of the sort of convection rolls seen in plan view (Figure 1), because of the side wall constraint on the fluid dynamics. The thickness of the cuvette is restricted by the need for visibility and contrast. Nevertheless, it was shown that deep-layer plumes do not stir the whole fluid, whereas in shallow layers, i.e. ≤4 mm, the whole fluid eventually participates in the convective motion.

When a culture in which a pattern has previously occurred is remixed, by shaking or swirling the container, the patterns disappear. The entire fluid system becomes cloudy due to scattering of the illumination from the now uniformly distributed cells. After the container is set down, the patterns reappear. The time for reconstituting the patterns depends on the cell and oxygen concentration, the duration and intensity of the mixing, and the depth of the fluid layer. Typically that time varies between 30 and 90 s. After the patterns reappear, it takes several minutes before they are nearly steady, and often much longer before a final state is reached. Increase of the cell concentration, by growth, is clearly not a factor in pattern generation.

Water filters were used, and light intensity was kept low, to avoid thermal convection. It was also necessary to cover the observing dish so as to avoid the generation of an evaporation-induced vertical temperature gradient.

Oxygen-taxis (actually aerotaxis) of the bacteria was demonstrated using a thin layer
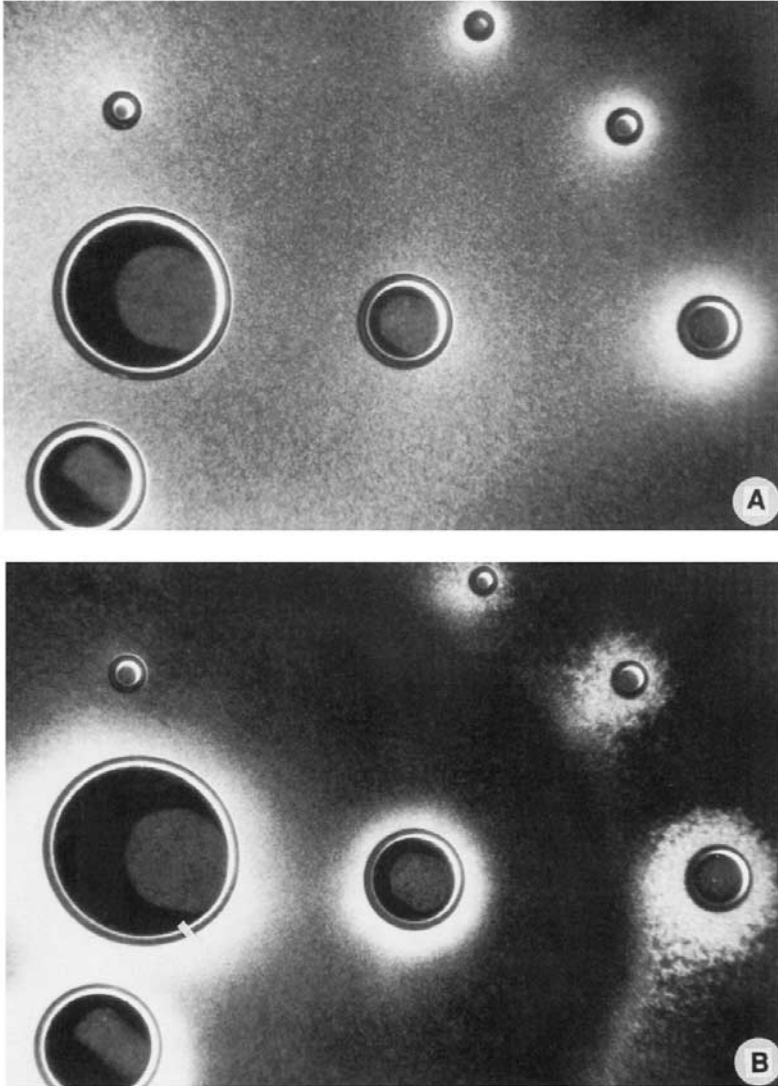
Figure 3. Oxygen-taxis of *Bacillus subtilis*. Plan view of fluid containing bacteria and air bubbles, located between glass surfaces. Dark-field illumination renders bacteria as white. The largest air bubble is ~1 mm in diameter. (A) Soon after the placement of the preparation on the microscope stage. Some bacteria have already swum towards the small peripheral bubbles. (B) Several minutes later. The spatial distribution of cells is essentially time-independent. The swarming bacteria are nearly close-packed around the bubbles.

of fluid bacterial culture between a microscope slide and a coverslip (Figure 3). Small air bubbles were trapped in the fluid. They eventually served to attract cells as the latter exhausted their oxygen supply, and oxygen diffused radially from the bubbles creating radial gradients. This test did not involve gravity or convection.

Another test of aerotaxis used the patterns themselves. It was found that when gas

access to the fluid was occluded by a cover slip floating on the surface, patterns vanished underneath the central region of the coverslip. Some of the patterns from beyond the coverslip steadily persisted approximately 1 mm under the edge of it. This observation indicated that the loss of patterns below the glass cover did not imply that they were driven by surface tension gradients.

In further tests we placed the bacterial culture in a nitrogen atmosphere. Initially there were some weak and unusual patterns, presumably due to dissolved oxygen effects. Unlike in the case of an air interface, the patterns vanished after a few minutes.

Patterns generated by motility mutants differed markedly from the normal ones, but not enough data are currently available.

TRANSPORT

A complete mathematical description of consumption-driven bioconvection patterns involves six conservation equations which link the fluid dynamics, the cell's swimming, and the supply, distribution and consumption of oxygen. Some of the required ingredients are unknown, particularly a detailed description of bacterial motility in an oxygen gradient. The fluid dynamical equations provide for calculations of the fluid velocity, $\mathbf{u}$, given a driving force. For bioconvection, the driving force is gravity, operating on local departures of the fluid density from the mean. Differences of density are directly proportional to variations of cell concentration. These variations arise from the interaction of the swimming cells' trajectories with guiding influences, such as chemical concentration gradients, and with the fluid's velocity. The fluid equations are well known (Pedley & Kessler, 1992) and are not presented here. They have been applied to calculations of algal bioconvection.

The equations that govern oxygen transport and consumption, and cell swimming, can be used to estimate characteristic lengths and times. These calculations are simple in the limiting cases when the fluid velocity is approximately zero, before onset of convection, and when it is vigorous, so that complete mixing becomes a reasonable assumption.

The conservation, consumption and transport of the oxygen concentration c (molecules cm^{-3}) is given by

$$\frac{\partial c}{\partial t} = D\nabla^2 c - \nabla \cdot (\mathbf{u}c) - \gamma\, n. \tag{1}$$

The bacterial consumption of oxygen is γ (molecules cell^{-1} s^{-1}), the diffusion coefficient is D (cm^2 s^{-1}) and the cell concentration is n (cells cm^{-3}). If only the vertical direction is of interest, $\nabla \to \partial/\partial z$. The fluid, velocity $\mathbf{u}$, transports oxygen, hence the flux term $\mathbf{u}c$ (molecules cm^{-2} s^{-1}). For cells, the analogous equation is

$$\frac{\partial n}{\partial t} = -\nabla \cdot [\mathbf{u} + \mathbf{V}(c)]n. \tag{2}$$

The swimming velocity $\mathbf{V}(c)$ is a function of c, its derivatives, and possibly a function of the history of c in the cells' reference frame. Both deterministic and stochastic motile behaviours are included (Pedley & Kessler, 1990) in $\mathbf{V}(c)$. When $c<c$(threshold), $\mathbf{V}(c)=0$. When c is large, $V(c)\approx V_b$. In a spatial gradient of c, $\mathbf{V}(c)$ is directed towards higher c, on average.

At the beginning of a typical experiment, the cuvette or petri dish which contains the cell culture is agitated until the cells are uniformly distributed, $n=n_o$, and the oxygen concentration is $c\approx c_o$, approximately the maximum solubility in equilibrium with air. After viscous damping causes the fluid velocity $\mathbf{u}$ to vanish, eqn 1 can be used to calculate consumption times and boundary layer thicknesses.

The bulk consumption time, T, can be calculated from eqn 1 by setting $D=0$. This procedure has validity because, as will be shown, the depth of the diffusion boundary layer that develops during T is much smaller than the dimensions of the bulk fluid. This means that after the deep-lying cells consume the initial oxygen concentration they are effectively cut off from supply.

Then, without diffusion,

$$c = c_o - \gamma\, n_0 t. \tag{3}$$

When $c=c_o/2$, $t\equiv T(1/2)=c_o/2\gamma n_o$. The approximate penetration depth, i.e. the diffusion boundary layer that develops during $T(1/2)$ is $L(1/2) = [2DT(1/2)]^{1/2} = [Dc_o/\gamma n_o]^{1/2}$. Using the estimates $\gamma=10^6$ molecules cell^{-1} s^{-1} (Berg, 1983), $n_o=10^9$ cm^{-3}, $D=2\times10^{-5}$ cm^2 s^{-1}, $c_o=1\cdot5\times10^{17}$ molecules cm^{-3}, one obtains $T(1/2)\approx75$ s and $L(1/2)\approx6\times10^{-2}$ cm. Thus, by the time half the oxygen is exhausted, the new supply from the air interface has hardly begun to penetrate. The usual depth of the fluid used in the experiments is ≥2 mm, which is considerably larger than $L(1/2)$. One may calculate L for other depletions of oxygen. For example, when all the oxygen is used up, $c=0$, $T=c_o/\gamma n_o$, and $L(0)=2^{1/2}L(1/2)$, or about 1 mm. Thus, the thickness of the boundary layer, and hence the penetration of oxygen to the bulk of the fluid, is not sensitive to the assumed total consumption.

Initially, all the bacteria are uniformly distributed in the fluid. The cells located near the air interface are the first to sense the oxygen gradient. As a result, they swim upwards, towards the interface. When their concentration is sufficient, convection begins as plumes that descend from the interfacial region. The observed time for plumes to start is of order one minute, and the depth of the layer out of which bacteria swim upwards is about 1 mm, both in agreement with the calculated T and L values. The bacteria-depleted layer shows up 'black' in dark-field illumination, so that the magnitude L can easily be estimated.

The boundary gradient of oxygen can also be calculated from steady conditions, assuming that eventually there is no time dependence of c. The bacteria then consume all the available oxygen which diffuses in from the top surface. Then $\partial c/\partial t=0$ in eqn 1. At $z=0$ the oxygen concentration is approximately in equilibrium with air, $c=c_o$, and at the bottom boundary the oxygen flux vanishes, $\partial c/\partial z=0$ at $z=H$. Then

$$\frac{c}{c_o} = 1 - \frac{\gamma\, n}{c_o D}\left[Hz - \frac{z^2}{2}\right]. \tag{4}$$

When $c/c_o=1/2$, $z(1/2)=c_0D/2\gamma nH=L(1/2)^2/2H$; $z(1/2)=0{\cdot}5\mathrm{x}10^{-2}$ cm for a typical value $H=3$ mm. The depth of the oxygen gradient is very shallow indeed. This calculation shows that the cell population, except for a thin surface layer, becomes anoxic in the absence of convective distribution of oxygen. The narrowness of the boundary means that it is unimportant to this calculation whether the cells and remaining oxygen in the main bulk of the fluid are stationary or well mixed, by bioconvection for example. There is, however, a big difference between the two. In the stationary case, the bacteria become anoxic and lose motility. In the convective case, the plumes and convection rolls continually pull pieces of the oxygenated boundary layer from the top surface into the bulk fluid, where they exchange places with the upward moving anoxic cell-containing streams. These regions of aerated fluid supply oxygen locally, and relatively slowly, with a characteristic time $T(1/2)$. It is this local aeration of the culture which maintains the observed motility of most of the cells in the population.

For the convective case, it can be argued that H, the depth where the flux is very small, should not be the total height of the cuvette, but some location in the moving fluid. One may set $z=H$ for some particular concentration, e.g. $c/c_o=0{\cdot}1$. Then $z(0{\cdot}1)=(9/5)\,L^{1/2}$, or about 1 mm, which corresponds to the size scale of some observed features of the convection.

It must be remembered that in the convective case both oxygen and bacteria are transported. Then both eqns 1 and 2 are required, with u supplied either from observations or the fluid mechanical equations. The rate of motion of the convection rolls can be experimentally determined by observing suspended particles. Preliminary measurements indicate $u\approx10^{-2}$ cm s^{-1}.

How do diffusion and convection compete over a distance R? A characteristic time for convective supply is $t_c=R/u$. For diffusion, the time is $t_d=R^2/D$. When the ratio $Pe=t_D/t_C=Ru/D$ is $\gg1$, the distribution process is dominated by convection, and conversely for $Pe\ll1$. For $u=10^{-2}$ and $D=2\mathrm{x}10^{-5}$, $Pe\equiv R\mathrm{x}10^3$. For $R>10^{-2}$ cm the long-range distribution of molecules is convective, but at small distances, e.g. in the gradient boundary layer, diffusion is dominant.

ENERGY BALANCE

The dissipation which accompanies any more or less steady convection pattern must be compensated by some source of energy. Since the system is isothermal, bacterial upward swimming, which generates gravitational potential energy, ought to be the only source of that energy. The gravitational potential energy per unit volume per second that is generated by n organisms per centimetre cubed, each organism having volume v and density, ρ_b, swimming in water with density, ρ_w is $vn(\rho_b-\rho_w)g\,V_{bu}$ (ergs s^{-1} cm^{-3}). The acceleration of gravity is g and the mean upward swimming speed of the bacteria is V_{bu}. The dissipation of energy per time per volume, due to viscosity and shear, which is the spatial variation of the fluid's velocity, $\mathbf{u}$, is $\mu(\mathrm{d}u/\mathrm{d}x)^2$ erg s^{-1} cm^{-3}. The derivative $\mathrm{d}u/\mathrm{d}x$ can be estimated by dividing the observed range of u by a typical wavelength scale of the pattern, determined by measuring the distance between adja-